

JOURNAL OF NEUROPHYSIOLOGY

October 1994
Volume 72, Number 4

Recru Select	4 Med 62 192	Pattern <i>realis</i>	1451
Neuro Preve Intrac	72 1994	Antagonists r	1464
Indep	7549-2268	ure	1476
Coor			1496
Identification of Molecular Components of A-Type Channels Activating at Subthreshold Potentials <i>P. Serôdio, C. Kentros, and B. Rudy</i>			1516
Glycine Response in Acutely Dissociated Ventromedial Hypothalamic Neuron of the Rat: New Approach With Gramicidin Perforated Patch-Clamp Technique <i>Y. Abe, K. Furukawa, Y. Itoyama, and N. Akaike</i>			1530
Blockade of NMDA-Activated Channels by Magnesium in the Immature Rat Hippocampus <i>G. J. Strecker, M. B. Jackson, and F. E. Dudek</i>			1538
Modulation of Ca ²⁺ -Channel Currents by Protein Kinase C in Adult Rat Sympathetic Neurons <i>Y. Zhu and S. R. Ikeda</i>			1549
Glutamate Metabotropic Receptors Increase a Ca ²⁺ -Activated Nonspecific Cationic Current in CA1 Hippocampal Neurons <i>V. Crépel, L. Aniksztejn, Y. Ben-Ari, and C. Hammond</i>			1561
Characteristics of Somatotopic Organization and Spontaneous Neuronal Activity in the Region of the Thalamic Principal Sensory Nucleus in Patients With Spinal Cord Transection <i>F. A. Lenz, H. C. Kwan, R. Martin, R. Tasker, R. T. Richardson, and J. O. Dostrovsky</i>			1570
The Synaptic Activation of N-Methyl-D-Aspartate Receptors in the Rat Medial Vestibular Nucleus <i>G. A. Kinney, B. W. Peterson, and N. T. Slater</i>			1588
The Learning of Novel Finger Movement Sequences <i>A. M. Gordon, A. Casabona, and J. F. Soechting</i>			1596
Adenosine Inhibition of Synaptic Transmission in the Substantia Gelatinosa <i>J. Li and E. R. Perl</i>			1611

(Continued)

Nicotinic and Muscarinic Activation of Motoneurons in the Crayfish Locomotor Network <i>D. Cattaert, A. Araque, W. Buño, and F. Clarac</i>	1622
Neural Responses Related to Smooth-Pursuit Eye Movements and Their Correspondence With Electrically Elicited Smooth Eye Movements in the Primate Frontal Eye Field <i>J. P. Gottlieb, M. G. MacAvoy, and C. J. Bruce</i>	1634
Vibration-Entrained and Premovement Activity in Monkey Primary Somatosensory Cortex <i>M. A. Lebedev, J. M. Denton, and R. J. Nelson</i>	1654
Interactions Between the Eye and Hand Motor Systems: Disruptions Due to Cerebellar Dysfunction <i>P. van Donkelaar and R. G. Lee</i>	1674
Intracellular pH Changes Produced by Glutamate Uptake in Rat Hippocampal Slices <i>A. Amato, L. Ballerini, and D. Attwell</i>	1686
Inhibition of Glutamate Release by Presynaptic κ_1 -Opioid Receptors in the Guinea Pig Dentate Gyrus <i>M. L. Simmons, G. W. Terman, C. T. Drake, and C. Chavkin</i>	1697
Developmental Regulation of Plasticity in Cat Somatosensory Cortex <i>S. L. Juliano, D. E. Eslin, and M. Tommerdahl</i>	1706
Network Interactions Among Limbic Cortices, Basal Forebrain, and Cerebellum Differentiate a Tone Conditioned as a Pavlovian Excitor or Inhibitor: Fluorodeoxyglucose Mapping and Covariance Structural Modeling <i>A. R. McIntosh and F. Gonzalez-Lima</i>	1717
Encoding of Amplitude and Rate of Forces Applied to the Teeth by Human Periodontal Mechanoreceptive Afferents <i>M. Trulsson and R. S. Johansson</i>	1734
Short-Term Homeostasis of Active Sleep and the Architecture of Sleep in the Rat <i>E. A. Vivaldi, A. Ocampo, U. Wyneken, M. Roncagliolo, and A. M. Zapata</i>	1745
Spread of Epileptiform Activity in the Immature Rat Neocortex Studied With Voltage-Sensitive Dyes and Laser Scanning Microscopy <i>B. Sutor, J. J. Hablitz, F. Rucker, and G. ten Bruggencate</i>	1756
Homosynaptic Facilitation of Transmitter Release in Crayfish Is Not Affected by Mobile Calcium Chelators: Implications for the Residual Ionized Calcium Hypothesis From Electrophysiological and Computational Analyses <i>J. L. Winslow, S. N. Duffy, and M. P. Charlton</i>	1769
Activity of Multiple Identified Motor Neurons Recorded Intracellularly During Evoked Feedinglike Motor Programs in <i>Aplysia</i> <i>P. J. Church and P. E. Lloyd</i>	1794
Coupling of Spinal Locomotor Networks in Larval Lamprey Revealed by Receptor Blockers for Inhibitory Amino Acids: Neurophysiology and Computer Modeling <i>A. Hagevik and A. D. McClellan</i>	1810
Distributed Actions and Dynamic Associations in Respiratory-Related Neuronal Assemblies of the Ventrolateral Medulla and Brain Stem Midline: Evidence From Spike Train Analysis <i>B. G. Lindsey, L. S. Segers, K. F. Morris, Y. M. Hernandez, S. Saporta, and R. Shannon</i>	1830

Spread of Epileptiform Activity in the Immature Rat Neocortex Studied With Voltage-Sensitive Dyes and Laser Scanning Microscopy

BERND SUTOR, JOHN J. HABLITZ, FRANZ RUCKER, AND GERRIT TEN BRUGGENCATE

Institute of Physiology, University of Munich, Munich, Germany

SUMMARY AND CONCLUSIONS

1. Adult rats and rats with a postnatal age of 3–29 days (PN 3–29) were used for the preparation of in vitro slices of the frontal neocortex. Epileptiform activity was induced by bath application of the γ -aminobutyric acid-A ($GABA_A$) receptor antagonists bicuculline or picrotoxin.

2. The voltage-sensitive dye RH 414 and a laser scanning microscope were used for multiple-site optical recordings of membrane potential changes associated with epileptiform activity. Optical signals were compared with simultaneously measured extracellular field potentials.

3. Optical signals could be reliably recorded for the duration of the experiments (2–4 h). Extracellular recordings of convulsant-induced paroxysmal depolarizing shifts (PDSs) in slices stained with RH 414 were comparable with those obtained in unstained slices. Changes in dye signals in response to reductions in extracellular calcium, addition of tetrodotoxin (TTX), or application of excitatory amino acid receptor antagonists indicate that the fluorescence changes correlate well with established electrophysiological measures of epileptiform activity.

4. In slices from adult animals, dye signals were observed at all recording sites. The response with the shortest latency occurred invariably at the site of stimulation, and activity spread rapidly in both vertical and horizontal directions. Spread was significantly faster in the vertical than in the horizontal direction.

5. Epileptiform activity was absent or only weakly expressed in slices from PN 3–9 animals. Activity was detectable predominantly in upper cortical layers.

6. Dye signals were observed at all measurement points in slices from PN 10–19 animals. In this age group, peak amplitude increased with spread of activity from lower to upper cortical layers. There was no significant difference between the speed of propagation in the vertical and in the horizontal directions. Spontaneous epileptiform activity occurred at a high rate in the PN 10–19 age group, and signals associated with spontaneous epileptiform events were largest in upper layers.

7. In the PN 10–19 age group, optical signals were characterized by the repetitive occurrence of PDS discharges superimposed on a sustained response. The amplitude of the sustained response decreased with increasing distance from the site of stimulation. Analysis of the latencies revealed that the superimposed PDS-like events were generated at multiple sites within the scanning area. Amplitude and rate of rise were largest in slices from PN 10–19 animals. These values declined with ongoing development.

8. The *N*-methyl-D-aspartate (NMDA)-mediated component of optically recorded epileptiform activity was determined by either subtraction of responses recorded in the presence of D-2-amino-5-phosphonovaleric acid (APV) from those taken under control conditions or by application of the non-NMDA receptor antagonist 6-cyano-7-nitroquinoxaline-2,3-dione (CNQX). The NMDA components obtained by these two procedures displayed slow rates of rise and different patterns of spatial distribution.

9. Our results demonstrate that the voltage-sensitive dye RH 414 can be used to reliably monitor the initiation, distribution,

and spread of convulsant-induced epileptiform activity in the rat neocortex in vitro. In PN 10–19 animals, epileptiform activity displays the highest degree of synchronization, which declines with ongoing development. The observation that activity can start from multiple sites in the tissue to form long-lasting ictal-like events that are not observed in adult animals suggests that the threshold for the initiation of epileptiform activity may be lower in the immature neocortex.

INTRODUCTION

The application of convulsant drugs to slices of the mature neocortex results in paroxysmal events that readily spread throughout the tissue (Chervin et al. 1988; Prince and Connors 1986). When recorded intracellularly, these paroxysmal events are characterized by large membrane depolarizations up to 500 ms in duration that give rise to burstlike discharges of action potentials (Gutnick et al. 1982; Lee and Hablitz 1991a). In the mature neocortex in vitro, these paroxysmal depolarizing shifts (PDSs) can be observed upon blockade of γ -aminobutyric acid ($GABA_A$) receptor-mediated inhibitory synaptic transmission (Connors 1984; Gutnick et al. 1982; Lee and Hablitz 1991a) or by an enhancement of *N*-methyl-D-aspartate (NMDA)-dependent excitatory postsynaptic potentials (EPSPs) after a reduction in the extracellular Mg^{2+} concentration (Avoli et al. 1987; Sutor and Hablitz 1987b). Independent of the mode of generation, PDSs can be greatly reduced or blocked by the application of excitatory amino acid receptor antagonists (Lee and Hablitz 1991a), indicating a dominant role for these receptors in the generation and maintenance of epileptiform activity in the mature neocortex.

During early postnatal development, the pattern of convulsant-induced epileptiform activity is age dependent (Hablitz 1987; Swann and Brady 1984). From postnatal day (PN) 0–5, immature neocortex and hippocampus are both incapable of generating PDS-like events comparable with those observed in mature tissue. In contrast, during the 2nd and 3rd wk of development, application of convulsants to neocortical or hippocampal slices leads to the occurrence of spontaneous and evoked epileptiform discharges that are enhanced compared with those observed in slices obtained from mature animals. These ictal-like discharges, lasting 5–10 s, consist of repetitive bursts accompanied by unusually large increases in the extracellular potassium activity (Hablitz and Heinemann 1987). Intracellular recordings have indicated that this epileptiform activity is due to a sustained synaptic input involving both NMDA and non-NMDA receptor-mediated components (Lee and Hablitz 1991b). Little is known, however, about the spread of epi-

leptiform activity in the rat neocortex in vitro at different stages of postnatal development.

The spread of epileptiform in the cortex has typically been investigated with the use of conventional electrophysiological techniques. Linear arrays of microelectrodes and subsequent current source density (CSD) analysis have been used to study laminar spread of epileptiform activity in vivo (Barth et al. 1990) and in vitro (Connors 1984). In both cases, epileptiform activity displayed a constant pattern of vertical spread through the neocortex. From the in vivo experiments (Barth et al. 1990), it was concluded that epileptiform activity is triggered in the supragranular layers, whereas the in vitro studies show (Connors 1984) that a population of bursting cells located in layer IV-V is responsible for the generation and synchronization of epileptiform activity. This discrepancy might be partly due to the lack of afferent fiber input in neocortical slices. In the adult neocortex the horizontal spread of epileptiform activity is controlled by GABA-mediated inhibition, and small reductions in inhibition result in a large increase in the spread of excitation (Chagnac-Amitai and Connors 1989a). Furthermore, the velocity of horizontal propagation of epileptiform discharges across the cortical mantle shows regional variability (Chervin et al. 1988). This periodicity might be related to variations in the length or density of horizontal excitatory connections.

Although these studies provided basic insights into the mechanisms of spread of epileptiform activity, the interpretation of their results is hampered by technical limitations. With the use of multiple microelectrodes, relatively few points can be used to study vertical and lateral spread. Linear electrode arrays provide the possibility to record simultaneously from a larger number of points in the tissue but have been used principally to study spread in the vertical direction. An alternative approach is the use of voltage-sensitive dyes to study the spatiotemporal distribution of epileptiform activity. Albowitz et al. (1990) performed optical recordings of voltage changes associated with epileptiform discharges in neocortical slices from adult animals. The spatiotemporal distribution of epileptiform discharges was independent of the convulsant applied, and epileptiform activity appeared to be generated in supragranular layers. Horizontal spread of activity was slower than in the vertical spread. Similar studies have not been performed in the developing brain.

Initial studies of initiation and propagation of epileptiform activity in the immature neocortex indicated that spontaneous events can arise from multiple areas and, once initiated, spread to adjacent cortical regions (Hablitz 1987; Wong and Prince 1990). However, the exact mechanisms involved in spread of activity and the patterns of spread are unclear. In the present study, we have used voltage-sensitive dyes and optical recording techniques to study the characteristics of the spatiotemporal distribution of epileptiform activity in the immature neocortex. Preliminary accounts of some of these findings have appeared (Sutor et al. 1992, 1993).

METHODS

Experiments were performed on brain slices prepared from the frontal cortex of 3- to 40-day-old Wistar rats. The procedure for

slice preparation was similar to the method described previously (Sutor and Hablitz 1989a). In brief, the animals were anesthetized with ether and decapitated. The brain was removed and stored for 30–60 s in ice-cold saline. Slices with a nominal thickness of 500 μ m were made with the use of a Vibroslice (Campden Instruments, UK). The slices were stored in oxygenated saline at room temperature for at least 1 h. Individual slices were transferred to the recording chamber where they were kept submerged between two nylon meshes and perfused with artificial cerebrospinal fluid (ACSF). The ACSF consisted of (in mM) 125 NaCl, 3 KCl, 2 CaCl_2 , 1.5 MgCl_2 , 1.25 NaH_2PO_4 , 25 NaHCO_3 , and 10 D-glucose. The solution was continuously gassed with a mixture of 95% O_2 -5% CO_2 , resulting in a pH of 7.4 at a recording temperature of 31–32°C.

A concentric bipolar stimulating electrode positioned at defined points within the scanning area (see below) was used to evoke normal and epileptiform activity. Threshold intensity was defined as the minimum stimulus strength necessary to evoke epileptiform activity with a constant latency. The stimulus duration was set to 50 μ s, and the maximal stimulus frequency was 1 per 2 min. To monitor the viability of the slices, extracellular recordings were routinely performed with the use of glass microelectrodes filled with 1 M NaCl. Intracellular recordings were made by means of microelectrodes filled with 3 M KCl. Epileptiform activity was induced by bath application of bicuculline methiodide (3–10 μ M) or picrotoxin (50 μ M). The convulsants were applied 30–50 min before recording commenced. Tetrodotoxin (TTX), 6-cyano-7-nitroquinoxaline-2,3-dione (CNQX), and D-2-amino-5-phosphonovaleric acid (APV) were added to the saline. To monitor spontaneous activity, the electrophysiologically recorded signals were displayed continuously on a chart recorder.

For measurement of activity-dependent optical signals, the slices were stained with the voltage-dependent fluorescent dye (*N*-(3-(triethylammonium)propyl)-4-(4-(p-diethylaminophenyl)butadienyl)pyridinium, dibromide (RH 414) (Grinvald et al. 1988). Staining of the slices was performed by recirculating perfusion of the slices for 1 h with saline containing 30 μ M RH 414. After this staining period, excess dye was washed out with normal saline for at least 30 min. Activity-dependent changes in fluorescence were detected with the use of a laser scanning microscope (Hiendl 1992). The experimental setup consisted of a recording chamber placed on the stage of an inverted microscope. Fluorescence was elicited by exciting the dye with light from a krypton laser (Innova 90 K, Coherent, Palo Alto, CA; wavelength: 530.9 nm). The emitted light was guided through a 590-nm cutoff filter and measured with the use of a single photodiode. A computer-controlled shutter was used to ensure that the laser light did not reach the preparation between measurements, thereby reducing toxic effects of the dye and errors due to dye bleaching. The optical signals were amplified with a DC coupled amplifier (bandwidth: 0–80 kHz) and stored on a computer. To compensate for slight instabilities in the laser output, a small part of the light from the laser beam (<5%) was directed onto a second (reference) photodiode by means of a dichroic mirror. The signal determined by the first photodiode was then divided by that obtained with the reference diode, thus correcting for any instabilities. Effects due to bleaching of the dye were corrected for by measurements taken in the absence of stimulation. The traces with evoked activity were then divided by these correction curves. All optical signals represent percent changes in fluorescence. In all figures a decrease in fluorescence is plotted as an upward deflection. As evaluated from simultaneously recorded field potentials, optical measurements could be performed for at least 2 h without significant deterioration of neuronal activity.

In these experiments 20 optical recording sites (channels) were arranged within a 1 \times 1 mm area of the neocortex as shown in Fig. 1. The correct arrangement of the points was controlled with the

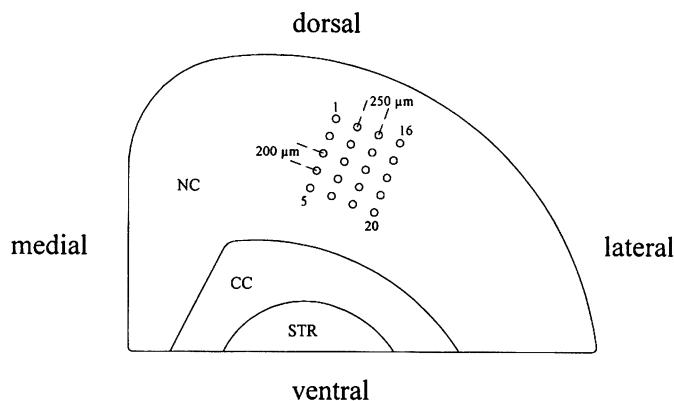


FIG. 1. Schematic diagram showing the appearance of the neocortical slice and the location of the recording sites. The scanning area and the slice are scaled similarly. NC, neocortex; CC, corpus callosum; STR, striatum.

use of a CCD video camera system. Each point had a diameter of 80 μm . The most dorsal point was placed 200–400 μm below the pial surface. In slices obtained from young animals (up to PN 12), this array covered the cortical layers II–V and part of layer VI. In slices from rats older than 14 days, the array covered layers II–V. The laser beam was guided from point to point by means of acousto-optical deflectors (Isomet, Springfield, VA). At sweep durations of 1 and 3 s, the sampling rate of the laser was 1 and 0.5 kHz per optical channel, respectively. A sampling rate of 1 kHz means that the laser cycled through all optical recording sites 1,000 times within 1 s resulting in a quasismultaneous recording of activity at each of the 20 points. To minimize bleaching and toxic effects, the maximum sweep duration was 3 s.

For analysis of evoked activity, two to three optically recorded sweeps were averaged, and the following parameters were determined: 1) latency to response onset (i.e., the time from stimulation to the 1st deviation from the baseline that exceeded 1 SD of the noise); 2) time-to-peak; 3) amplitude; and 4) rate of rise (the fastest rate of rise of the response was approximated by linear regression and is given in units of $\%s^{-1}$). Results are expressed as mean \pm SE. Statistical analysis was performed with the use of unpaired 2-tailed *t*-tests or an analysis of variance (ANOVA) for repeated measures.

RESULTS

Optical measurements of epileptiform activity

Recordings were obtained from neocortical slices of 31 immature rats between PN 3 and PN 30 and from slices of 12 adult animals (>30 days). Initial experiments were performed to validate the use of voltage-sensitive dyes to study the spread of epileptiform activity in the immature neocortex. In all experiments, extracellular field potential recordings indicated that the application of bicuculline or picrotoxin resulted in the induction of epileptiform activity. In stained slices, electrical stimulation evoked epileptiform field potentials (Fig. 2*A*), which were similar to those obtained in slices not stained with RH 414 (Fig. 2*C*), indicating that the dye did not alter the tissue's ability to generate epileptiform activity. The time course and amplitude of the epileptiform field potentials were also similar in stained and unstained slices. Figure 2*D* shows an intracellular recording from a PN 20 animal. In the presence of 10 μM bicuculline, electrical stimulation in layer IV evoked a PDS. The epileptiform field potential depicted in Fig. 2*C* was ob-

tained immediately after withdrawal of the electrode from the cell. Simultaneous extracellular and optical recordings (Fig. 2, *A* and *B*) revealed that epileptiform field potentials were accompanied by decreases in fluorescence (Fig. 2*B*). The time course of the optical signal was similar to that of extra- and intracellularly recorded PDSs. With the use of the voltage-sensitive dye RH 414, a decrease in fluorescence corresponds to a depolarization of the membrane potential (Grinvald et al. 1988). Both epileptiform field potentials and the associated optically detected changes in fluorescence were blocked by application of TTX (0.6 μM) or by reduction in the extracellular Ca^{2+} concentration to 0.2 mM.

The results described above indicate that the signals obtained by using optical recording techniques reflect epileptiform activity. This was further evaluated by examining the effect of changes in strength of synaptic activation and by investigating the actions of the NMDA and non-NMDA receptor antagonists APV and CNQX. Increases in stimulus strength are known to decrease the latency to PDS onset without affecting amplitude or duration (Lee and Hablitz 1991a). The effect of changes in stimulus strength on optical signals is shown in Fig. 3. Recordings from four sites within the recording array are shown, and the responses to stimuli of 175 and 470 μA are superimposed. It can be seen that increasing the stimulus strength decreased the latency, especially in superficial layers, and increased the rate of rise of the responses. Peak amplitude and duration (not shown) were not significantly altered. Intracellular recordings from immature neocortical neurons have shown that bath application of the non-NMDA receptor antagonist CNQX abolishes or greatly reduces evoked epileptiform discharges (Lee and Hablitz 1991b). In the present experiments, addi-

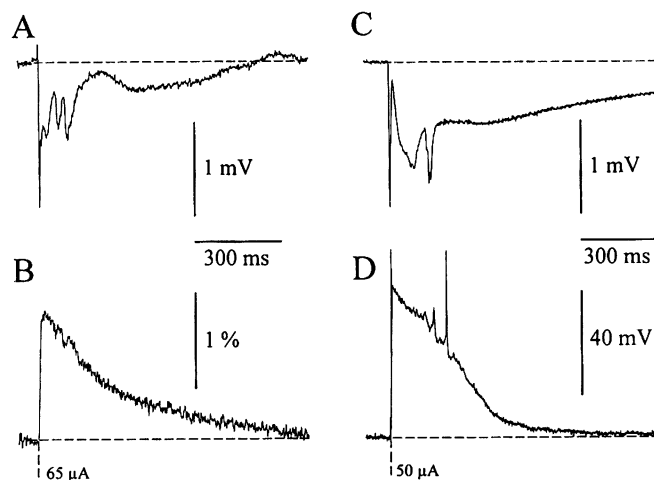


FIG. 2. Comparison of intra- and extracellular recordings with optically detected signals. *A*: measurement of an epileptiform field potential in a RH 414-stained slice. Bicuculline (10 μM) was applied to induce epileptiform activity. *B*: simultaneously recorded optical signal at the same site in the slice. *C*: extracellular field potential recording obtained from an unstained slice in the presence of bicuculline. Record was taken after electrode was withdrawn from cell shown in *D*. *D*: intracellular recording of a paroxysmal depolarizing shift (PDS) in a postnatal day (PN) 20 neocortical neuron. The resting membrane potential was -76 mV, and the input resistance was 43 M Ω . Traces in *A*–*C* represent averages of 3 single sweeps each, whereas this in *D* is a single response. The dashed vertical lines in *B* and *D* indicate the time of stimulation.

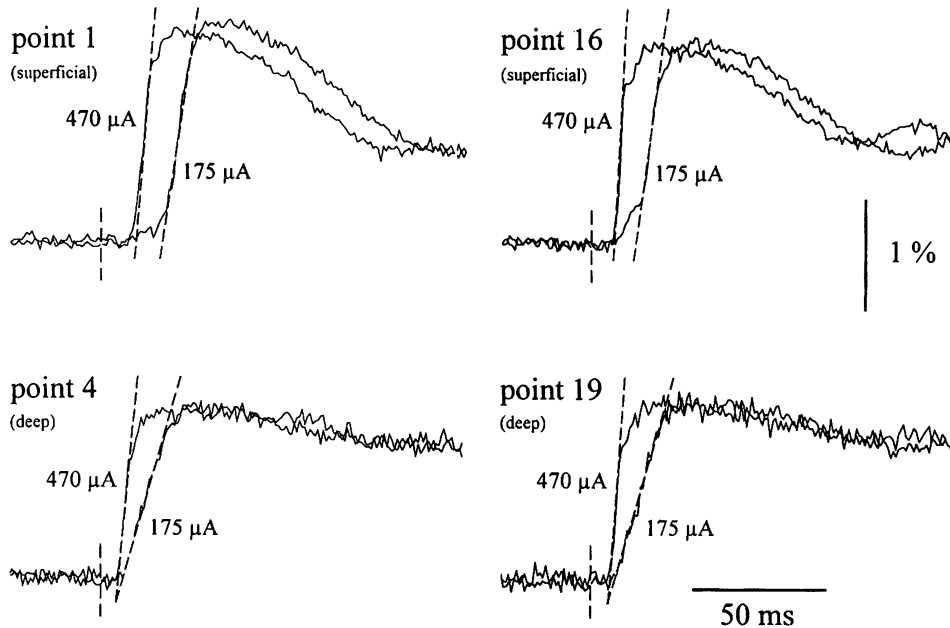


FIG. 3. Effects of changes in stimulus strength on evoked optical signals. Recordings were taken in the presence of 50 μ M picrotoxin from 4 sites within the recording array. Numbers refer to the points described in Fig. 1. Stimulation was adjacent to point 15. Records obtained at 2 stimulus strengths are shown superimposed for each recording site. Dashed lines indicate where linear regression lines were fitted for rate of rise determinations.

tion of CNQX (5–10 μ M) led to an inhibition of epileptiform activity (see Fig. 11, *A* and *B*). This effect was observed in all slices tested ($n = 13$), independent of the age of the animal. By analogy to results obtained from intracellular recordings (Lee and Hablitz 1991b), the NMDA receptor antagonist APV (10–20 μ M) reduced the amplitude of the late component of the optically recorded PDS (see Fig. 10*A*) in all slices tested ($n = 18$). These results suggest that optical signals accurately assess the neuronal activity responsible for epileptiform activity in the immature brain.

Characteristics of optically recorded epileptiform activity in slices from adult rats

An example of optical signals associated with evoked epileptiform activity in an adult slice is shown in Fig. 4. Stimulation occurred near point 10 within the scanning area, and the recording sites were arranged as shown in Fig. 1. A characteristic feature of optically recorded epileptiform activity in adult animals was that dye signals were observed at all recording sites. The shortest latency of response was invariably measured at the site of stimulation. Starting from this point, the activity spread rapidly in both horizontal and vertical directions. The mean velocity of spread in the vertical direction was significantly faster ($0.131 \pm 0.028 \text{ ms}^{-1}$, mean \pm SE, $n = 6$) than that in the horizontal plane ($0.078 \pm 0.023 \text{ ms}^{-1}$, $n = 6$, $P < 0.02$). The amplitudes of the signals were smaller in the deeper cortical layers and increased by $19 \pm 8\%$ ($n = 7$) with spread to more superficial regions of the neocortex (Fig. 4). Similarly, the rate of rise of the signals increased from $4.5 \pm 2.0\% \text{ s}^{-1}$ to $18.2 \pm 6.9\% \text{ s}^{-1}$ ($n = 6$) with spread from deeper to superficial layers of the cortex. The difference between these two values was statistically significant ($P < 0.01$). This spatially dependent increase in rate of rise resulted in a constant time-to-peak of the signals, despite an increasing response latency (Fig. 4). The changes in the rate of rise with spread of activity from lower to upper layers was not specific for this age group,

being observed at all stages of development (see Figs. 10*B* and 12*A*).

Spread of epileptiform activity in slices from immature animals

PN 3–9. Previous work in the immature neocortex has shown that during the first postnatal week the threshold for evoking normal synaptic activity is high (Burgard and Hablitz 1993) and that epileptiform activity is difficult to evoke or absent (Hablitz 1987). In the present study, paroxysmal activity was absent or only weakly expressed in slices from animals in the PN 3–9 group. Figure 5 shows simultaneous optical recordings of neuronal activity from 19 different points in a slice from a PN 7 animal. In the presence of 10 μ M bicuculline, stimulation at point 20 (i.e., in lower layers of the cortex) evoked detectable activity predominantly in the upper cortical layers. The stimulus intensities necessary to elicit these responses were two to three times larger than those used in older rats. The epileptiform activity observed in this age group could be blocked by the non-NMDA receptor antagonist CNQX (5–10 μ M, $n = 3$) or by TTX (0.6 μ M, $n = 2$).

PN 10–19. Within the developmental period from PN 10 to 19, convulsant-induced epileptiform activity was recorded at all measurement points. As described previously by using extra- and intracellular recording techniques, activity in this age group consists of an initial PDS followed by a sustained depolarization with multiple superimposed late PDSs (Hablitz 1987). An example of an optical recording of such activity in a slice from a PN 18 animal is shown in Fig. 6. In the presence of 10 μ M bicuculline, threshold stimulation at point 20 led to large optical signals at all 20 recording sites. The shortest latency was measured at point 20, i.e., at the site of stimulation, and latencies increased with distance from the stimulation site. These results suggest that paroxysmal activity started at point 20 and spread throughout the slice (see Fig. 7*C*). The velocity of spread in

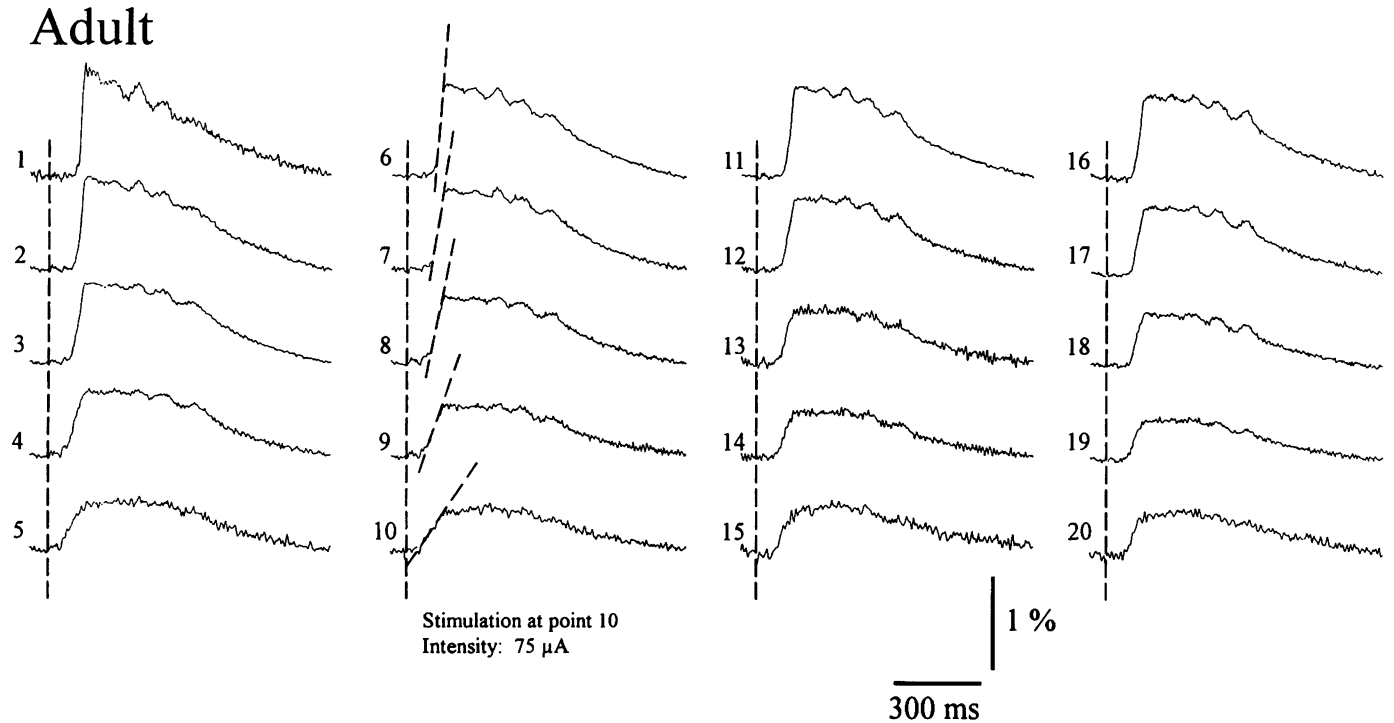


FIG. 4. Example of a simultaneous 20-site measurement of optical signals in a slice from an adult animal. Epileptiform activity was evoked in the presence of $10 \mu\text{M}$ bicuculline by electrical stimulation at point 10 with the use of an intensity of $75 \mu\text{A}$. Responses shown are the averages of 3 trials. Vertical lines indicate the time of stimulation. The additional dashed lines in recordings 6–10 represent the regression lines fitted to determine the rate of rise.

the vertical direction was $0.18 \pm 0.12 \text{ ms}^{-1}$ ($n = 9$) and $0.12 \pm 0.09 \text{ ms}^{-1}$ ($n = 9$) in the horizontal direction. These values are not significantly different from those obtained in adult rats. However, in contrast to adult animals, there was no significant difference between the velocities of spread in vertical and horizontal direction in this age group.

Similar to adult animals, the peak amplitude of the signals detected in the PN 10–19 age group increased with spread of activity from lower to upper cortical layers (Fig. 6). However, this increase was more pronounced than that observed in adult rats. At PN 10–19, the mean amplitude of the signals recorded in superficial cortical layers was found

PN 7

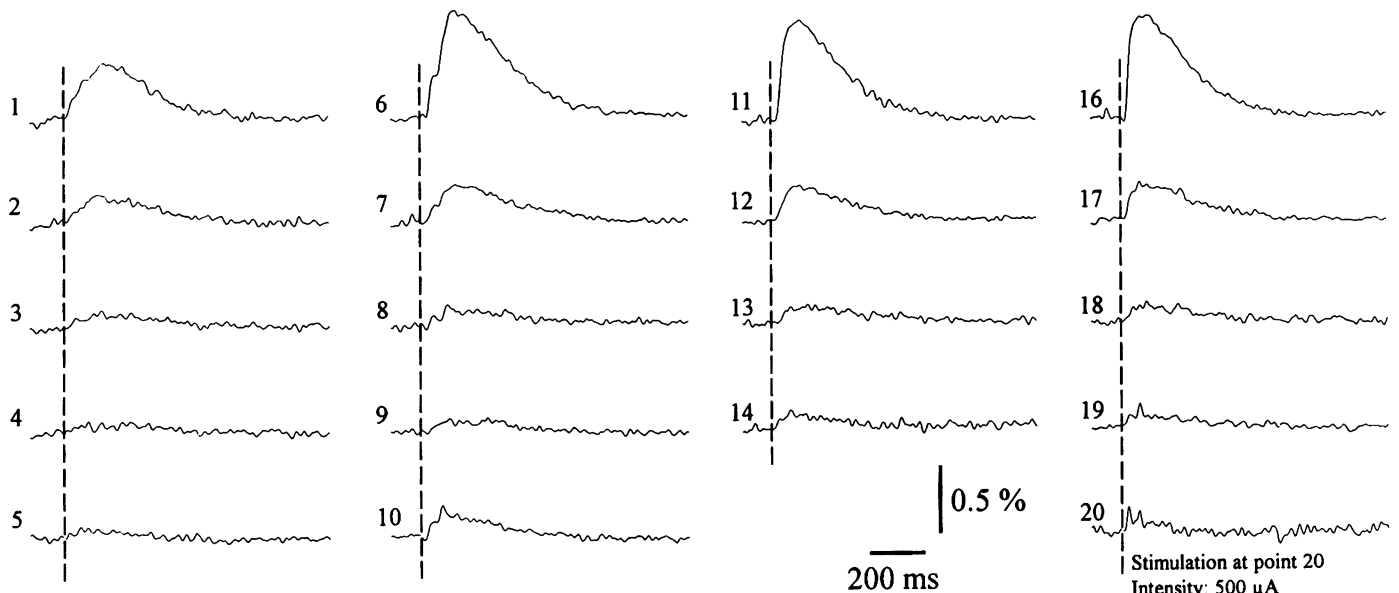


FIG. 5. Multiple site optical recordings in a slice from a PN 7 animal. Epileptiform activity was evoked by stimulation near point 20. Bicuculline ($10 \mu\text{M}$) was added to the saline. Activity was present at all recording sites in the top cortical layers but was only weakly expressed in the bottom layers.

PN 18

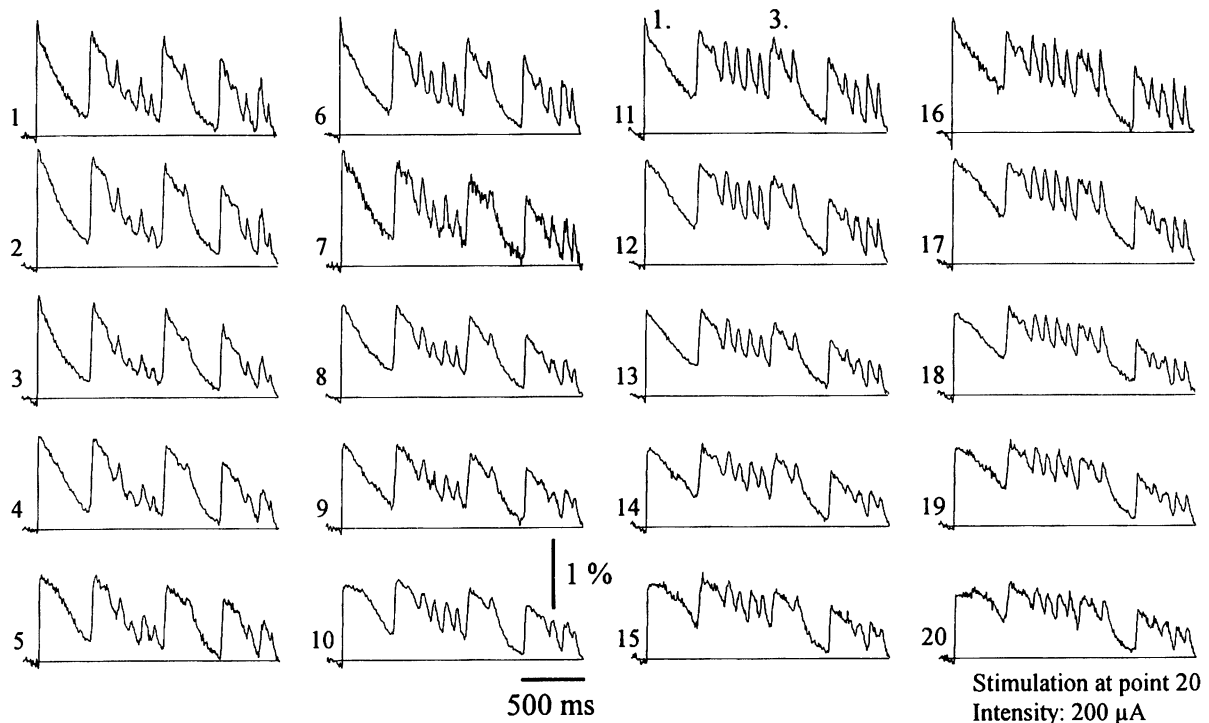


FIG. 6. Changes in optical signals associated with ictal-like paroxysmal discharges in a slice from a PN 18 animal. A single stimulus near site 20 ($200 \mu\text{A}$) evoked a long-lasting, ictal-like epileptiform discharge. Horizontal lines indicate baseline. Note the more prominent sustained component near the site of stimulation and the longer intervals between successive transients at sites 1–5 compared with sites 16–20.

to be increased by $78 \pm 34\%$ as compared with those observed in deeper layers.

The optically recorded responses observed in the PN 10–19 age group resembled those described previously with the use of intracellular recordings (Hablitz 1987). After a fast rising initial response, the signals declined but did not reach the baseline (Fig. 6). Instead, an additional decrease in fluorescence appeared, indicating that another depolarizing event had occurred. This sequence could repeat itself several times and last for 5–10 s, as could be seen from the simultaneous extracellular recordings. It was apparent that recording sites distal to the stimulation electrode showed longer delays between subsequent peaks. Moreover, a sustained response component present in points 16–20 became less prominent at distal sites (Fig. 6, compare points 16–20 to points 1–5).

To quantify the spread of activity, measurements of latency to onset were determined for two different peaks in the response (denoted 1. and 3. in the signal recorded at point 11 in Fig. 6) and plotted as a function of the recording site. Figure 7, *A* and *B*, shows the results from an experiment performed in a slice from a PN 12 rat. The latency to onset of the initial response was shortest near the site of stimulation (Fig. 7*A*, point 20) and increased with distance from point 20, both vertically and horizontally. For analysis of the second peak in the response, the site with the shortest initial latency was assigned a latency of zero, and signals recorded at the other points are described in terms of latencies relative to this site. It can be seen that, for the second response, the shortest latency was observed at point

5, and the relative latencies were prolonged with increasing distance from this point, suggesting that activity originated at point 5 (Fig. 7*B*). Figure 7, *C* and *D*, presents similar data from a recording in a PN 18 animal (Fig. 6). Activity was evoked by a stimulus near point 20, and the shortest latency response was observed at that site. In this case the shortest latency of the third peak in the optical signal was chosen for analysis and found to be at site 16. Starting from this point, the activity spread throughout the scanning area. These results suggest that the long-lasting epileptiform responses observed in the PN 10–19 age group are due to the superimposition of repetitive PDSs that are generated at multiple sites in the neocortex.

A principal feature of the PN 10–19 age group was the frequent (1–3/min) occurrence of spontaneous epileptiform discharges. Figure 8*A* shows an example of spontaneous discharges recorded in a slice from a PN 12 animal in the presence of bicuculline. Similar to evoked activity, the amplitude and rate of rise of the spontaneous signals were larger in the upper layers compared with those in lower layers. The responses labeled 1 and 2 in the *top* trace were chosen for latency analysis. According to the latency measurements of peak 1 (Fig. 8*B*), the activity started at point 10 and was detectable within the whole scanning area. Activity spread in both medial and lateral directions but appeared more synchronous in the lateral direction (note similarity of onset latencies at sites 16–20). However, spread was more rapid in the medial direction as indicated by the shorter latencies. The analysis of the latencies of the second peak in the response again indicated a more rapid spread in

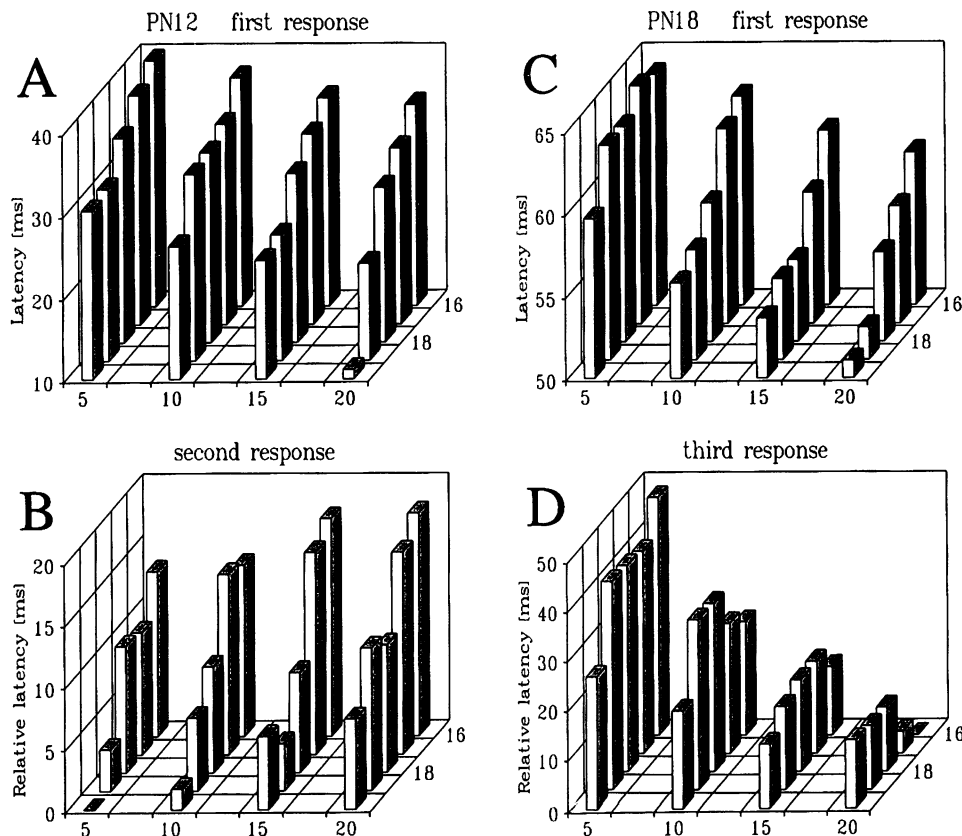


FIG. 7. Analysis of latencies of 1st and subsequent peaks of optical signals associated with ictal-like epileptiform discharges. *A* and *B*: results from a PN 12 animal. *C* and *D*: data from a PN 18 rat. *A* and *C*: latency to onset of the 1st response is plotted as a function of recording site. *B* and *D*: relative latencies of the 2nd and 3rd response, respectively, are depicted.

the medial direction but a greater synchronization across the depths of the cortex in the lateral direction (Fig. 8C).

PN 20–29. When compared with the age group PN 10–19, bicuculline- or picrotoxin-induced epileptiform activity observed in slice from 20- to 29-day-old rats displayed qualitatively similar characteristics. The main differences between these two age groups were smaller signal amplitudes and rates of rise in the older animals (see below). Especially, the frequency of spontaneous epileptiform events decreased to ~ 1 per 2 min. However, because spontaneous activity was almost absent in slices from adult rats, the PN 20–29 age group could be clearly distinguished from mature animals.

Developmental changes in optical signals

To compare epileptiform activity in different age groups, the mean amplitude and rate of rise in upper and lower layers of the cortex was determined. This was done by averaging responses at sites 5, 10, 15, and 20 (bottom layers), and sites 1, 6, 11, and 16 (top layers). The resulting values were then plotted as a function of age (Fig. 9). It can be seen that epileptiform activity was absent or poorly expressed in the youngest age group (PN 3–9). Furthermore, the strongest expression of bicuculline- or picrotoxin-induced epileptiform activity was observed in the age group of PN 10–19. At this postnatal age, the response amplitudes detected in the top cortical layers were about twice as large as those recorded from slices of adult rats (Fig. 9A). The signal amplitudes observed in the bottom layers were always smaller than those recorded in superficial layers, and there was no significant developmental change of these amplitudes (Fig. 9A). In the age group PN 10–19, the rate of rise of signals

recorded in the top and bottom cortical layers were 6 and 10 times larger, respectively, than those seen in mature animals. With increasing postnatal age, both the amplitude and rate of rise gradually declined, and the differences between the top and bottom cortical layers diminished. The developmental changes in the amplitude (upper layers) and the rate of rise of optically recorded epileptiform activity were statistically significant (ANOVA, $P < 0.001$ for amplitude and rate of rise of signals from superficial layers and $P < 0.05$ for rate of rise of signals from bottom layers).

Distribution of NMDA-mediated activity in the PN 10–19 age group

As already mentioned, intracellularly recorded PDSs can be reduced in amplitude and duration by application of the NMDA receptor antagonist APV. We therefore examined the effects of APV on optical signals and determined the NMDA-mediated component by subtracting signals recorded in the presence of APV from responses obtained before application of the antagonist. Figure 10, *A* and *B*, shows specimen records from top and bottom cortical layers, respectively, in the absence and presence of APV. In all slices tested ($n = 3$), APV ($20 \mu\text{M}$) reduced the amplitudes of the optical responses by 30–60%. After subtraction, the latency to onset and the rate of rise of the NMDA-mediated components were analyzed. Compared with control recordings, the response latencies were found to be 5–7 ms longer with no apparent spatial pattern. The rising phase of the NMDA-mediated component was significantly less steep than that of the signals recorded in the absence of

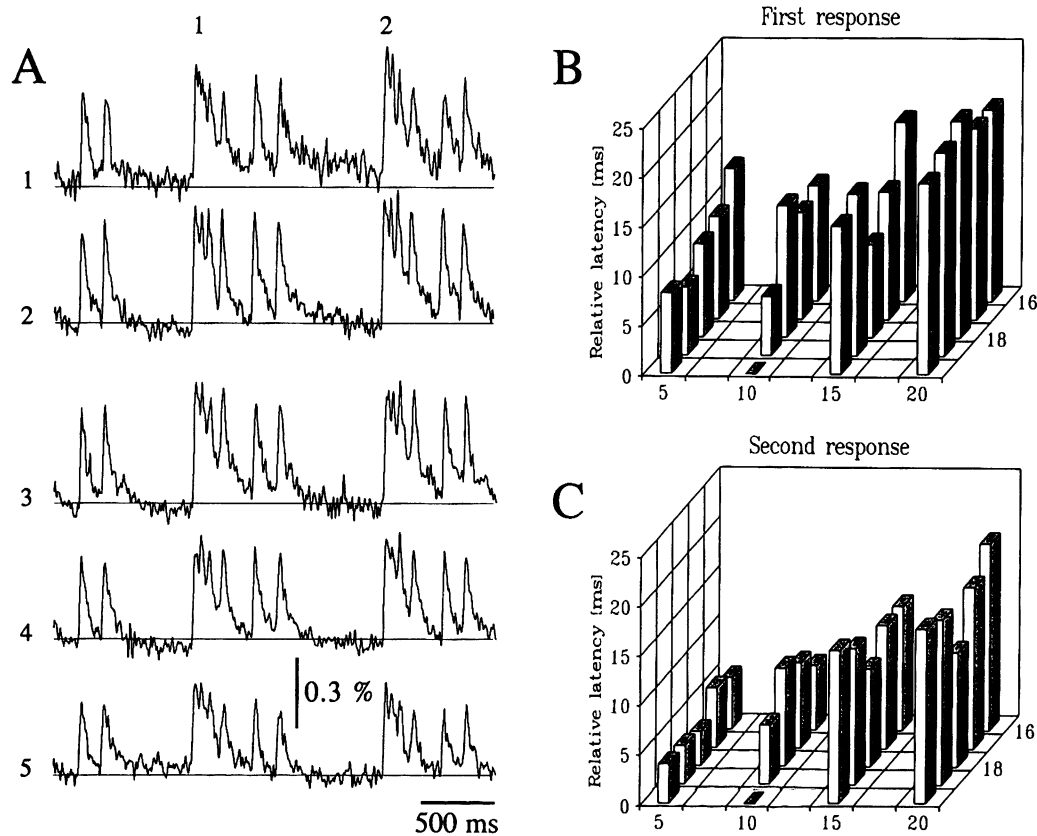


FIG. 8. Example of optical changes associated with spontaneous epileptiform activity in a slice from a PN 12 animal. *A*: specimen records of optical signals from sites 1–5. Numbers above trace from site 1 indicate responses measured for plots in *B* and *C*. *B*: plot of the relative latency of the wave labeled 1 in *A* as a function of recording site. *C*: similar to *B* but latencies of response 2 are plotted.

APV (Fig. 10, *B* and *C*), suggesting that this NMDA-mediated activity contributes more to the late components of the epileptiform responses without significantly influencing the initial time course of the signal (see superimposed signals in Fig. 10*A*). However, the spatial distribution of the rate of rise values remained unaffected in the presence of APV. The rate of rise of this NMDA-mediated component increased with spread from bottom to top layers (Fig. 10*C*).

After the application of the non-NMDA receptor antagonist CNQX (5–10 μ M), evoked epileptiform activity was suppressed when threshold intensity stimulation was used (Fig. 11, *A* and *B*). Upon an increase in stimulus strength to 2–4 times threshold intensity, optical signals could be recorded, even in the presence of CNQX (Fig. 11*C*). Such activity was subsequently blocked by APV application (Fig. 11*D*). Similar to the results obtained above by subtraction, the rate of rise of this NMDA-mediated component was found reduced compared with control values (Fig. 12, *A* and *B*). However, in contrast to the NMDA component isolated by subtraction (Fig. 10, *B* and *C*), the spatial distribution of the rate of rise values were different from those determined under control conditions (Fig. 12, *A* and *C*) and recording site independent. The slow rates of rise resulted in an increase in the measured times-to-peak, particularly in top layers (Fig. 12, *B* and *D*). This is an additional indication that NMDA receptor-mediated potentials contribute to the later parts of PDS discharges.

DISCUSSION

Our results demonstrate that the voltage-sensitive dye RH 414 can be used to reliably monitor the initiation, distribution, and spread of convulsant-induced epileptiform activity in the rat neocortex *in vitro*. The laser-scanning recording technique employed allowed reproducible detection of optical signals without serious photobleaching or toxicity. The changes in the dye signals in response to alterations in extracellular calcium, addition of TTX, or application of excitatory amino acid receptor antagonists indicate that the fluorescence changes correlate well with established electrophysiological measures of epileptiform activity. In addition, the optical recording method offered the possibility of simultaneous multisite measurements of both vertical and horizontal spread of paroxysmal events.

Origin of optical signals

The properties of styryl dyes such as RH 414 have been thoroughly examined (Cinelli and Kauer 1992; Cohen et al. 1978; Grinvald et al. 1988). These dyes bind to the external plasma membrane and change fluorescence in response to alterations in transmembrane voltage. The response kinetics of the dyes are fast enough to resolve individual action potentials (Chien and Pine 1991; Cohen et al. 1974), and the temporal resolution is usually limited by the recording system. In the present experiments the detection system had a wide recording bandwidth, and the sampling rate

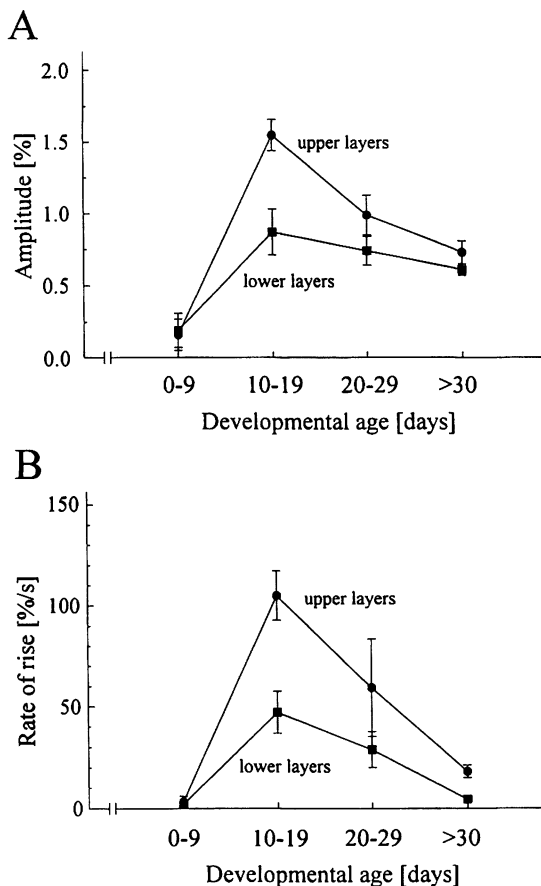


FIG. 9. Developmental changes in amplitude (*A*) and rate of rise (*B*) of optical signals. Results for top (points 1, 6, 11, and 16) and bottom (points 5, 10, 15, and 20) cortical layers are plotted separately. Values represent means \pm SD of 5–12 slices.

used permitted reliable detection of signals up to 460 Hz. Recordings performed at higher digitization rates (up to 2 kHz) revealed that the optical signals were not filtered by the sampling procedure. Thus the relatively slow optical signals recorded in the present experiments reflect voltage-dependent changes in fluorescence associated with epileptiform activity. This is substantiated by the comparison of the time course of extracellularly recorded paroxysmal events and optically registered signals. When recorded simultaneously at the same site in the tissue, both signals had similar time courses (see Fig. 2).

For the interpretation of optical recordings, it is important to consider that voltage-sensitive dyes monitor different aspects of neuronal activity than intra- or extracellular recordings. Intracellular recordings, in combination with pharmacological and biophysical manipulations, provide precise information concerning changes in membrane and synaptic potentials of individual cells during paroxysmal events. Extracellularly recorded field potentials represent the extracellular current flow resulting from the summated activity of a population of cells. Optical signals also reflect summated activity. However, the observed signal is the outcome of the summation of transmembrane voltage changes at cellular membranes. Each point over which optical measurements were taken covered an area of $\sim 5,026 \mu\text{m}^2$. When using a slice with a nominal thickness of $500 \mu\text{m}$, the

resulting volume of tissue contains multiple cellular elements, including dendrites and cell bodies of both neurons and glia, and activity from elements at different depths in the slice will be summated. Because multiple elements contribute to the optical signals, their exact origin is unclear. However, because the optical signals were blocked by TTX, by the non-NMDA receptor antagonist CNQX and by reductions in the extracellular Ca^{2+} concentration, it is reasonable to assume that this activity resulted predominantly from depolarizations associated with synaptic events, intrinsic membrane conductances, and glial cells. However, it is not possible to exactly determine the contribution of glial cells to the optical signals. Measurements of changes in extracellular potassium concentration (Hablitz and Heinemann 1987; B. Sutor, unpublished observations), which is the main stimulus for glial depolarization, have shown that these responses reach their maximum after the initial PDS has occurred. Therefore glial cells are not likely to contribute significantly to the peak amplitude or the rate of rise of the signals, i.e., the parameters chosen to quantitatively analyze epileptiform activity.

Because optical signals represent summated activity of a population of cells, response magnitude can be considered as a relative measure of the number of cells involved in the generation of the signal and, indirectly, reflects the degree of synchronization of activity. In addition to neuronal synchrony, the amplitude of the signals depends on the amount of dye bound per membrane area and the density of membranes within the recording area. As pointed out by Albowitz et al. (1990), membrane density is larger in superficial layers compared with deeper layers. Therefore, if a constant amount of dye bound per membrane area is assumed, the signals in superficial layers could be expected to be inherently larger than those in deeper layers. In fact, such an amplitude distribution has been observed in the present experiments (see Fig. 4). However, we believe that differences in membrane densities do not significantly influence the spatial signal amplitude distribution. In a given cortical layer, significantly larger optical signals were observed during early postnatal periods when the overall membrane surface is smaller than in mature tissue (Miller 1988).

Another parameter indicating the degree of synchronization of a population of neurons is the rate of rise of the optical signals. The rate of rise of extracellularly recorded field EPSPs in the dentate gyrus or in the stratum radiatum of the hippocampus is considered to be an indicator of synaptic strength (Andersen et al. 1978; Lomo 1971). With increasing stimulus intensity, the rate of rise of the field EPSPs increases, thereby synchronizing the action-potential discharge of the neurons. The rate of rise of the optically recorded epileptiform responses displayed a similar behavior. Because these optical signals reflect the summated activity of a large number of cells, their rate of rise should be useful as a measure of neuronal synchronization.

Ontogenetic changes in optical signals

The results presented show that optical signals display a developmental pattern similar to that reported with the use of electrical recording techniques (Hablitz 1987). Activity was difficult to evoke or not present in PN 3–9 animals;

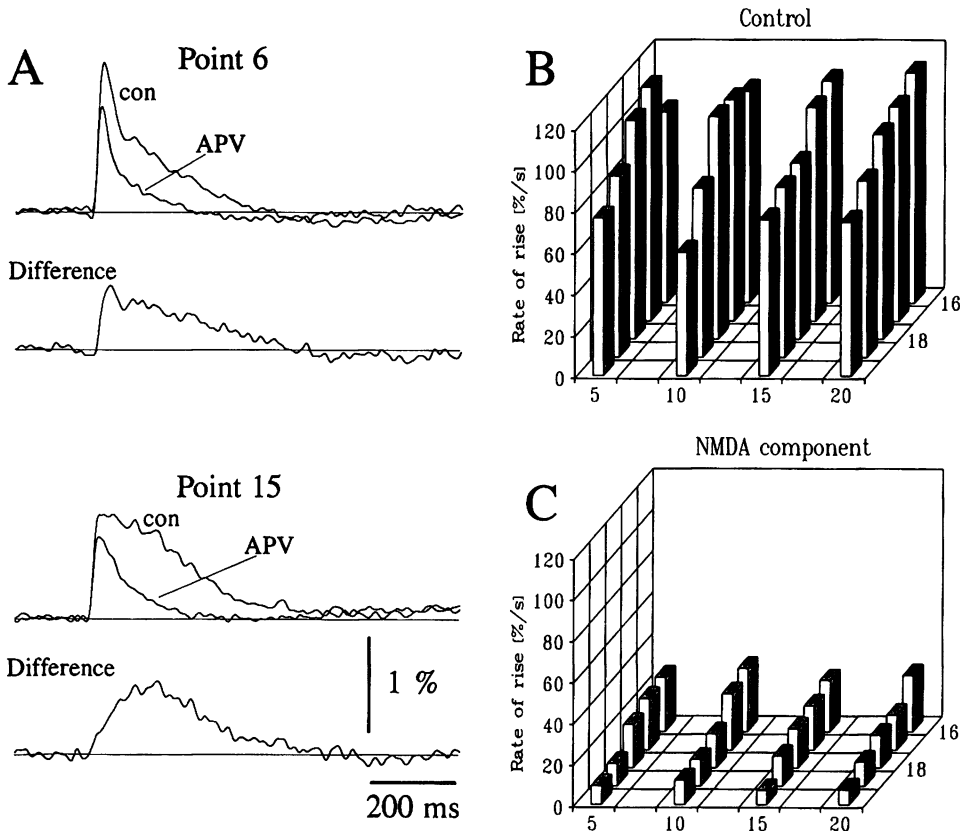


FIG. 10. Distribution of optical signals mediated by *N*-methyl-D-aspartate (NMDA) receptors in a PN 15 animal. *A*: specimen records from top (point 6) and lower (point 15) cortical layers before (con) and after (APV) bath application of 10 μ M D-2-amino-5-phosphonovaleric acid (APV) are shown superimposed. Digital subtraction of the 2 traces yielded the response shown below. *B*: plot of the spatial distribution of the rate of rise under control conditions. *C*: the spatial distribution of the rate of rise of the difference signals obtained by digital subtraction (NMDA component).

spontaneous, ictal-like events were observed in the PN 10–19 group; and an adultlike pattern was seen at ages >30 days. Both NMDA and non-NMDA receptors contribute to epileptiform discharges in the immature neocortex (Lee and Hablitz 1991b). A similar sensitivity to excitatory amino acid-receptor antagonists was observed in the optical recordings.

During the early postnatal period (PN 3–9), the neocortex is undergoing rapid changes in anatomic and physiological organization. Golgi studies have demonstrated that synaptic contacts are sparse (Miller 1988). Electrophysiological studies have shown that evoked EPSPs are present in the

PN 3–8 age group. The elicitation of these potentials requires high stimulus strengths, and they were unable to follow stimulation at rates >0.1 Hz (Burgard and Hablitz 1993; Kriegstein et al. 1987). By the second postnatal week, neocortical neurons display well-defined basal and apical dendritic structures, and EPSPs have taken on a more adultlike pattern. Our inability to consistently evoke epileptiform activity in the PN 3–9 group may indicate a lack of sufficient excitatory connections to permit the synchronization of a neuronal population. Traub et al. (1987) have shown that the number of recurrent excitatory synaptic connections can influence the propagation of epileptiform

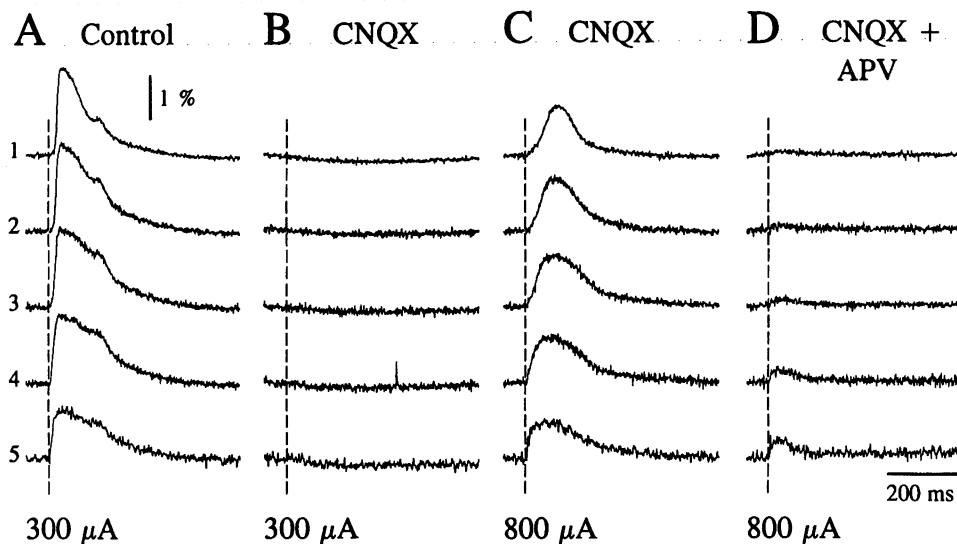


FIG. 11. Effects of glutamate receptor antagonists on epileptiform activity recorded in a slice from a PN 15 animal. *A–D*: specimen records from sites 1–5. Epileptiform activity was induced by application of picrotoxin (50 μ M). *A*: responses under control condition evoked by stimulation with an intensity of 300 μ A. *B*: 6-cyano-7-nitroquinoxaline-2,3-dione (CNQX; 5 μ M) suppressed the activity. *C*: in the presence of CNQX, an increase in stimulus strength to 800 μ A elicited optical responses at all recording sites. *D*: this activity was blocked by application of APV (20 μ M).

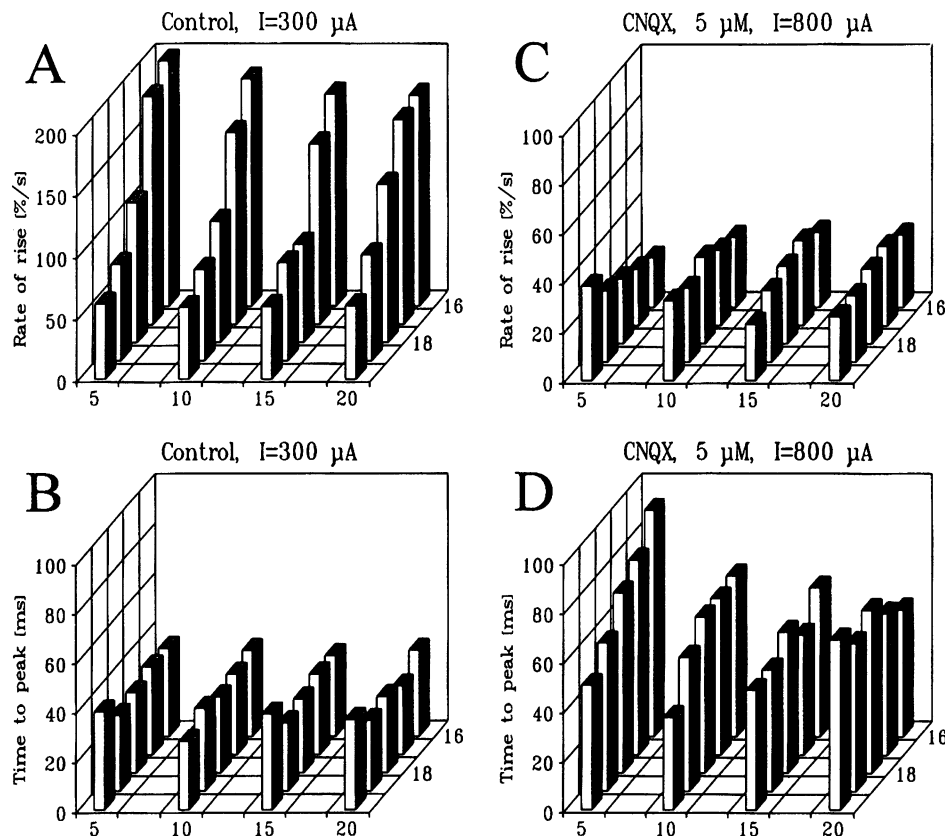


FIG. 12. Spatial distribution of the rates of rise (*A* and *C*) and times to peak (*B* and *D*) of the experiment shown in Fig. 11. The corresponding values are plotted as a function of the recording site. *A*: distribution of the rate of rise of the signals in the presence of picrotoxin (50 μ M, control). Stimulus intensity was 300 μ A. *B*: distribution of the times-to-peak under the same experimental conditions. *C*: spatial pattern of the rates of rise in the presence of picrotoxin and CNQX (5 μ M) at a stimulus intensity of 800 μ A. *D*: plot of the time-to-peak as a function of recording site. Experimental conditions similar to *C*.

activity. It appears that a critical number of such connections must be present before the neocortex can display sustained epileptiform activity.

In the age groups older than PN 9, a characteristic pattern of spread of evoked activity was observed. The responses with the shortest latencies invariably occurred at the site of stimulation, and activity spread in both horizontal and vertical directions. In slices from adult animals, the speed of propagation was faster in the vertical than in the horizontal direction. This difference was not observed in slices from PN 10–19 animals. In this age group, the velocity of spread was the same in both directions. This finding might be explained by delayed development of GABA_B-mediated post-synaptic inhibition. Fukuda et al. (1993) reported that GABA_B receptor-mediated IPSPs were only rarely observed in PN 7–17 animals. Reduced GABA_B-mediated inhibition can intensify epileptiform activity (Scanziani et al. 1991; Sutor and Luhmann 1992) and might facilitate the horizontal propagation of epileptiform activity at earlier developmental stages. Spread from deeper to top layers probably reflects the activity of synapses formed by vertically running, presumably intrinsic, cortical fibers. Horizontal spread across column boundaries must involve local connections formed by axon collaterals of pyramidal cells. These fibers are known to travel for millimeters in the neocortex (Martin 1984). The difference in the rate of spread of activity in vertical versus horizontal directions may, in addition, reflect a greater density of collaterals in the neonate, as observed in the immature hippocampus (Swann et al. 1992). Such horizontally oriented collaterals may underlie the ictal-like discharges seen during this developmental period.

A major finding of the present experiments is that both amplitude and rate of rise of the evoked responses progressively decrease during development. Maximum values were observed at PN 10–19. At this stage, there was also a greater distinction between top and bottom layers compared with adult animals. The larger response amplitudes in slices from PN 10–19 animals indicate that more cellular elements were involved in its generation or that the potential changes in neurons and glia cells were more pronounced or both. The steeper rate of rise of the responses detected in slices from younger age groups probably represents a greater degree of synchronization. Epileptiform activity in the developing neocortex is accompanied by unusual large increases in extracellular potassium (Hablitz and Heinemann 1987). Measurements of the laminar distribution of changes in potassium activity associated with epileptiform activity at different developmental stages revealed that potassium activity reaches its highest values in the top layers in slices of the PN 10–19 age group (Sutor, unpublished observations). These changes in the extracellular potassium activity could facilitate the synchronization of neuronal activity. The incidence of electrotonic coupling between neocortical neurons is also significantly higher in younger animals (Connors et al. 1983; Peinado et al. 1993). Electrical transmission between cortical neurons via gap junctions could contribute significantly to synchronization of paroxysmal activity.

The vertical distribution of field potentials in the center of well-established cortical epileptic foci in vivo has been described in several studies (Elger et al. 1981; Gumnit et al. 1970; Petsche et al. 1978). Negative field potentials occur in all cortical laminae with maximal amplitudes observed

in layer V. Similar results have been described in vitro experiments (Connors 1984). When the convulsant agent penicillin is applied to discrete cortical layers, epileptiform activity develops most rapidly after an injection into layer IV (Chatt and Ebersole 1982). Neurons in deep layer IV and upper layer V are known to display intrinsic burst properties (McCormick et al. 1985) and distinct morphological characteristics (Chagnac-Amitai et al. 1990). These observations have given rise to the hypothesis that a network of intrinsically bursting neurons located in middle cortical layers initiate synchronous epileptiform activity (Chagnac-Amitai and Connors 1989b; Gutnick et al. 1982). However, neurons with intrinsic bursting properties are not seen before PN 14 (Franceschetti et al. 1993). Evidence also exists that during seizure activity superficial layers may become active independently. Petsche et al. (1978) have shown changes in cortical amplitude profiles during seizures, whereas Albowitz et al. (1990) found that the amplitude of delayed epileptiform potentials were always largest in layer III. Similarly, in the present study, the optical signals with the largest amplitudes were also observed in upper cortical layers. These results suggest that local excitatory interactions in layer III (Langdon and Sur 1990) may be important for epileptogenesis and serve as a means for amplification of epileptiform discharges. Analysis of optical signals associated with spontaneous activity or evoked events with repetitive discharges indicated that epileptiform activity could start at multiple sites within the recording array. These results suggest that different populations of neuronal elements contribute to epileptiform discharges at different times during an ictal-like event and that the degree of synchronization during such an event is variable.

Distribution of NMDA-mediated components of epileptiform activity

Similar to results obtained in electrophysiological experiments, a decrease in the amplitude and duration of optically recorded epileptiform signals was observed after application of the NMDA receptor antagonist APV. When the NMDA-mediated components were isolated, either by subtraction or by application of CNQX, the rates of rise of these components appeared slower than that of the control responses. Therefore it seems unlikely that NMDA receptors contribute significantly to the initial phase of the optically recorded signals. Because the NMDA channels display a current-voltage relationship that is similar to that of regenerative conductances, it can be assumed that NMDA receptors influence the magnitude of epileptiform activity by amplifying the responses. The effects of APV were found to be more pronounced in the upper cortical layers, suggesting that amplification of epileptiform activity may occur predominantly in these layers.

This work was supported by the Deutsche Forschungsgemeinschaft (SFB 220/TP 10) and NS22373.

Permanent address: J. J. Hablitz, Neurobiology Research Center and Department of Physiology and Biophysics, University of Alabama at Birmingham, Birmingham, AL 35294.

Received 25 February 1994; accepted in final form 28 June 1994.

REFERENCES

- ALBOWITZ, B. AND KUHN, U. Spatio-temporal distribution of epileptiform potentials in the hippocampal slice: recordings with voltage-sensitive dyes. *Eur. J. Neurosci.* 3: 570–586, 1991.
- ALBOWITZ, B., KUHN, U., AND EHRENREICH, L. Optical recording of epileptiform voltage changes in the neocortical slice. *Exp. Brain Res.* 81: 241–256, 1990.
- ANDERSEN, P., SILFVENIUS, H., SUNDBERG, S. H., SYEEN, O., AND WIGSTROM, H. Functional characteristics of unmyelinated fibers in the hippocampal cortex. *Brain Res.* 144: 11–18, 1978.
- AVOLI, M., LOUVEL, J., PUMAIN, R., AND OLIVIER, A. Seizure-like discharges induced by lowering $[Mg^{2+}]$ in the human epileptogenic neocortex maintained in vitro. *Brain Res.* 417: 199–203, 1987.
- BARTH, D. S., BAUMGARTNER, C., AND DI, S. Laminar interactions in rat motor cortex during cyclical excitability changes of the penicillin focus. *Brain Res.* 508: 105–117, 1990.
- BURGARD, E. C. AND HABLITZ, J. J. Developmental changes in NMDA and non-NMDA receptor-mediated synaptic potentials in rat neocortex. *J. Neurophysiol.* 69: 230–240, 1993.
- CHAGNAC-AMITAI, Y. AND CONNORS, B. W. Horizontal spread of synchronized activity in neocortex and its control by GABA-mediated inhibition. *J. Neurophysiol.* 61: 747–758, 1989a.
- CHAGNAC-AMITAI, Y. AND CONNORS, B. W. Synchronized excitation and inhibition driven by intrinsically bursting neurons in neocortex. *J. Neurophysiol.* 62: 1149–1162, 1989b.
- CHAGNAC-AMITAI, Y., LUHMANN, H. J., AND PRINCE, D. A. Burst generating and regular spiking Layer 5 pyramidal neurons of rat neocortex have different morphological features. *J. Comp. Neurol.* 296: 598–613, 1990.
- CHAT, A. B. AND EBERSOLE, J. S. The laminar sensitivity of cat striate cortex to penicillin induced epileptogenesis. *Brain Res.* 241: 382–387, 1982.
- CHERVIN, R. D., PIERCE, P. A., AND CONNORS, B. W. Periodicity and directionality in the propagation of epileptiform discharges across neocortex. *J. Neurophysiol.* 60: 1695–1713, 1988.
- CHIEN, C. B. AND PINE, J. Voltage-sensitive dye recording of action potentials and synaptic potentials from sympathetic microcultures. *Biophys. J.* 60: 697–711, 1991.
- CINELLI, A. R. AND KAUFER, J. S. Voltage-sensitive dyes and functional activity in the olfactory pathway. *Annu. Rev. Neurosci.* 15: 321–351, 1992.
- COHEN, L. B., SALZBERG, B. W., DAVILA, H. V., ROSS, W. N., LANDOWNE, D., WAGGONER, A. S., AND WANG, C. H. Changes in axon fluorescence during activity: molecular probes of membrane potential. *J. Membr. Biol.* 19: 1–36, 1974.
- COHEN, L. B., SALZBERG, B. W., AND GRINVALD, A. Optical methods for monitoring neuron activity. *Annu. Rev. Neurosci.* 1: 171–182, 1978.
- CONNORS, B. W. Initiation of synchronized neuronal bursting in neocortex. *Nature Lond.* 310: 685–687, 1984.
- CONNORS, B. W., BENARDO, L. S., AND PRINCE, D. A. Coupling between neurons of the developing rat neocortex. *J. Neurosci.* 3: 773–782, 1983.
- EAYRS, J. T. AND GOODHEAD, B. Postnatal development of the cerebral cortex in the rat. *J. Anat.* 93: 385–402, 1959.
- ELGER, C. E., SPECKMANN, E.-J., PROHASKA, O., AND CASPERS, H. Pattern of intracortical potential distribution during focal interictal epileptiform discharges (FIED) and its relation to spinal field potentials in the rat. *Electroencephalogr. Clin. Neurophysiol.* 51: 393–402, 1981.
- FRANCESCHETTI, S., BUZIO, S., SANCINI, G., PANZICA, F., AND AVANZINI, G. Expression of intrinsic bursting properties in neurons of maturing sensorimotor cortex. *Brain Res.* 162: 25–28, 1993.
- FUKUDA, A., MODY, I., AND PRINCE, D. A. Different ontogenesis of presynaptic and postsynaptic GABA_B inhibition in rat somatosensory cortex. *J. Neurophysiol.* 70: 448–452, 1993.
- GRINVALD, A., FROSTIG, R. D., LIEKE, E. E., AND HILDESHEIM, R. Optical imaging of neuronal activity. *Physiol. Rev.* 68: 1285–1366, 1988.
- GUMNIT, R. J., MATSUMOTO, H., AND VASCONETTO, C. DC activity in the depth of an experimental epileptic focus. *Electroencephalogr. Clin. Neurophysiol.* 28: 333–339, 1970.
- GUTNICK, M. J., CONNORS, B. W., AND PRINCE, D. A. Mechanisms of neocortical epileptogenesis in vitro. *J. Neurophysiol.* 48: 1321–1335, 1982.
- HABLITZ, J. J. Spontaneous ictal-like discharges and sustained potential

- shifts in the developing rat neocortex. *J. Neurophysiol.* 58: 1052–1065, 1987.
- HABLITZ, J. J. AND HEINEMANN, U. Extracellular K^+ and Ca^{2+} changes during epileptiform discharges in the immature rat neocortex. *Dev. Brain Res.* 36: 299–303, 1987.
- HIENDL, R. *Untersuchungen zur optischen Erfassung neuronaler Aktivität mittels Objektastastung durch einen Laserstrahl* (PhD thesis). Munich, Germany: Technical University of Munich, 1992.
- KONNERTH, A., ORKAND, P. M., AND ORKAND, R. K. Optical recording of electrical activity from axons and glia of frog optic nerve: potentiometric dye responses and morphometrics. *Glia* 1: 225–232, 1988.
- KRIEGSTEIN, A. R., SUPPES, T., AND PRINCE, D. A. Cellular and synaptic physiology and epileptogenesis of developing rat neocortical neurons in vitro. *Dev. Brain Res.* 34: 161–171, 1987.
- LANGDON, R. B. AND SUR, M. Components of field potentials evoked by white matter stimulation in isolated slices of primary visual cortex: spatial distributions and synaptic order. *J. Neurophysiol.* 64: 1484–1501, 1990.
- LEE, W. L. AND HABLITZ, J. J. Initiation of epileptiform activity by excitatory amino acid receptors in the disinhibited rat neocortex. *J. Neurophysiol.* 65: 87–95, 1991a.
- LEE, W. L. AND HABLITZ, J. J. Excitatory synaptic involvement in epileptiform bursting in the immature rat neocortex. *J. Neurophysiol.* 66: 1894–1901, 1991b.
- LØMO, T. Patterns of activation in a monosynaptic cortical pathway: the perforant path input to the dentate area of the hippocampal formation. *Exp. Brain Res.* 12: 18–45, 1971.
- LONDON, J. A., COHEN, L. B., AND WU, J. Y. Optical recordings of the cortical response to whisker stimulation before and after the addition of an epileptogenic agent. *J. Neurosci.* 9: 2182–2190, 1989.
- MARTIN, K. A. C. Neuronal circuits in cat striate cortex. In: *Cerebral Cortex. Functional Properties of Cortical Cells*, edited by E. G. Jones and A. Peters. New York: Plenum, 1984, vol. 2, p. 241–284.
- MCCORMICK, D. A., CONNORS, B. W., LIGHTHALL, J. W., AND PRINCE, D. A. Comparative electrophysiology of pyramidal and sparsely spiny stellate neurons of the neocortex. *J. Neurophysiol.* 54: 782–806, 1985.
- MILLER, M. W. Development of projection and local circuit neurons in neocortex. In: *Cerebral Cortex. Development and Maturation of Cerebral Cortex*, edited by A. Peters and E. G. Jones. New York: Plenum, 1988, vol. 7, p. 133–175.
- PEINADO, A., YUSTE, R., AND KATZ, L. C. Extensive dye coupling between rat neocortical neurons during the period of circuit formation. *Neuron* 10: 103–114, 1993.
- PETSCHKE, H., MÜLLER-PASCHINGER, I. B., POCKBERGER, H., PROHASKA, O., RAPPELSBERGER, P., AND VOLLMER, R. Depth profiles of electrocortical activities and cortical architectonics. In: *Architectonics of the Cerebral Cortex*, edited by M. A. B. Brazier and H. Petsche. New York: Raven, 1978, p. 257–280.
- PRINCE, D. A. AND CONNORS, B. W. Mechanisms of interictal epileptogenesis. In: *Advances in Neurology*, edited by A. V. Delgado-Escueta, A. A. Ward, Jr., D. M. Woodbury, and R. J. Porter. New York: Raven, 1986, vol. 44, p. 275–299.
- SCANZIANI, M., GÄHWILER, B. H., AND THOMPSON, S. M. Paroxysmal inhibitory potentials mediated by GABA_B receptors in partially disinhibited rat hippocampal slice cultures. *J. Physiol. Lond.* 444: 375–396, 1991.
- SUTOR, B. AND HABLITZ, J. J. Excitatory postsynaptic potentials in rat neocortical neurons in vitro. I. Electrophysiological evidence for two distinct EPSPs. *J. Neurophysiol.* 61: 607–620, 1989a.
- SUTOR, B. AND HABLITZ, J. J. Excitatory postsynaptic potentials in rat neocortical neurons in vitro. II. Involvement of *N*-methyl-D-aspartate receptors in the generation of EPSPs. *J. Neurophysiol.* 61: 621–634, 1989b.
- SUTOR, B. AND LUHMANN, H. Modulation of convulsant-induced epileptiform activity in rat neocortical slices by the GABA-B receptor antagonist CGP 35348. *Pfluegers Arch.* 420, Suppl. 1: R16, 1992.
- SUTOR, B., RUCKER, F., TEN BRUGGENCATE, G., AND HABLITZ, J. J. Spread of epileptiform activity monitored by voltage-sensitive dyes in the immature neocortex. *Epilepsia* 33, Suppl. 3: 21–22, 1992.
- SUTOR, B., HABLITZ, J. J., RUCKER, F., AND TEN BRUGGENCATE, G. Spread of epileptiform activity in the developing rat neocortex. *Pfluegers Arch.* 422, Suppl. 1: R17, 1993.
- SWANN, J. W. AND BRADY, R. J. Penicillin-induced epileptogenesis in immature rat CA3 hippocampal pyramidal cells. *Dev. Brain Res.* 12: 243–254, 1984.
- SWANN, J. W., SMITH, K. L., GOMEZ, C. M., AND BRADY, R. J. The ontogeny of hippocampal local circuits and focal epileptogenesis. In: *Molecular Neurobiology of Epilepsy*, edited by J. Engel, Jr., C. Wasterlain, E. A. Cavalheiro, U. Heinemann, and G. Avanzini. Amsterdam: Elsevier, *Epilepsy Res. Suppl.* 9, 1992, p. 115–126.
- TRAUB, R. D., KNOWLES, W. D., MILES, R., AND WONG, R. K. S. Models of the cellular mechanism underlying propagation of epileptiform activity in the CA2-CA3 region of the hippocampal slice. *Neuroscience* 21: 457–470, 1987.
- WONG, B. Y. AND PRINCE, D. A. The lateral spread of ictal discharges in neocortical brain slices. *Epilepsy Res.* 7: 29–39, 1990.